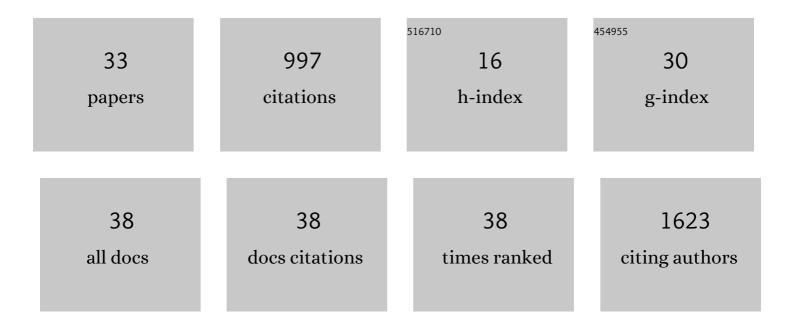
## Elias P Rosen

List of Publications by Year in descending order

Source: https://exaly.com/author-pdf/254218/publications.pdf Version: 2024-02-01



FLINS P POSEN

#	Article	IF	CITATIONS
1	Drugâ€Dependent Morphological Transitions in Spherical and Worm‣ike Polymeric Micelles Define Stability and Pharmacological Performance of Micellar Drugs. Small, 2022, 18, e2103552.	10.0	31
2	Mass Spectroscopy Imaging of Hair Strands Captures Short-Term and Long-Term Changes in Emtricitabine Adherence. Antimicrobial Agents and Chemotherapy, 2022, 66, e0217621.	3.2	7
3	Antiretroviral drug exposure in lymph nodes is heterogeneous and drug dependent. Journal of the International AIDS Society, 2022, 25, e25895.	3.0	8
4	Poly(2-oxazoline) nanoparticle delivery enhances the therapeutic potential of vismodegib for medulloblastoma by improving CNS pharmacokinetics and reducing systemic toxicity. Nanomedicine: Nanotechnology, Biology, and Medicine, 2021, 32, 102345.	3.3	32
5	Quantitative Imaging Analysis of the Spatial Relationship between Antiretrovirals, Reverse Transcriptase Simian-Human Immunodeficiency Virus RNA, and Collagen in the Mesenteric Lymph Nodes of Nonhuman Primates. Antimicrobial Agents and Chemotherapy, 2021, 65, .	3.2	6
6	Using Real-Time Adherence Feedback to Enhance Communication About Adherence to Antiretroviral Therapy: Patient and Clinician Perspectives. Journal of the Association of Nurses in AIDS Care, 2020, 31, 25-34.	1.0	11
7	Application of a Scavenger Receptor A1-Targeted Polymeric Prodrug Platform for Lymphatic Drug Delivery in HIV. Molecular Pharmaceutics, 2020, 17, 3794-3812.	4.6	9
8	Influence of hair treatments on detection of antiretrovirals by mass spectrometry imaging. Analyst, The, 2020, 145, 4540-4550.	3.5	6
9	Infrared Matrix-Assisted Laser Desorption Electrospray Ionization Mass Spectrometry Imaging of Human Hair to Characterize Longitudinal Profiles of the Antiretroviral Maraviroc for Adherence Monitoring. Analytical Chemistry, 2019, 91, 10816-10822.	6.5	17
10	Heterogeneous antiretroviral drug distribution and HIV/SHIV detection in the gut of three species. Science Translational Medicine, 2019, 11, .	12.4	38
11	SCIDOT-03. HYPERLOADED POLY(2-OXAZOLINE) MICELLES AS PERSONALIZED DRUG CARRIERS FOR BRAIN TUMORS. Neuro-Oncology, 2019, 21, vi272-vi273.	1.2	1
12	scRNA-seq in medulloblastoma shows cellular heterogeneity and lineage expansion support resistance to SHH inhibitor therapy. Nature Communications, 2019, 10, 5829.	12.8	77
13	Antiretroviral Penetration across Three Preclinical Animal Models and Humans in Eight Putative HIV Viral Reservoirs. Antimicrobial Agents and Chemotherapy, 2019, 64, .	3.2	15
14	Patient and clinician perspectives on optimizing graphical displays of longitudinal medication adherence data. Patient Education and Counseling, 2019, 102, 1090-1097.	2.2	13
15	Antiretroviral concentrations and surrogate measures of efficacy in the brain tissue and CSF of preclinical species. Xenobiotica, 2019, 49, 1192-1201.	1.1	30
16	Evaluation of Digital Image Recognition Methods for Mass Spectrometry Imaging Data Analysis. Journal of the American Society for Mass Spectrometry, 2018, 29, 2467-2470.	2.8	18
17	Simian Immunodeficiency Virus Persistence in Cellular and Anatomic Reservoirs in Antiretroviral Therapy-Suppressed Infant Rhesus Macaques. Journal of Virology, 2018, 92, .	3.4	49
18	Virological and Immunological Responses to Raltegravir and Dolutegravir in the Gut-Associated Lymphoid Tissue of HIV-Infected Men and Women. Antiviral Therapy, 2018, 23, 495-504.	1.0	6

ELIAS P ROSEN

#	Article	IF	CITATIONS
19	Analysis of Antiretrovirals in Single Hair Strands for Evaluation of Drug Adherence with Infrared-Matrix-Assisted Laser Desorption Electrospray Ionization Mass Spectrometry Imaging. Analytical Chemistry, 2016, 88, 1336-1344.	6.5	40
20	Influence of C-Trap Ion Accumulation Time on the Detectability of Analytes in IR-MALDESI MSI. Analytical Chemistry, 2015, 87, 10483-10490.	6.5	17
21	Mass Spectrometry Imaging Reveals Heterogeneous Efavirenz Distribution within Putative HIV Reservoirs. Antimicrobial Agents and Chemotherapy, 2015, 59, 2944-2948.	3.2	67
22	Quantitative mass spectrometry imaging of emtricitabine in cervical tissue model using infrared matrix-assisted laser desorption electrospray ionization. Analytical and Bioanalytical Chemistry, 2015, 407, 2073-2084.	3.7	66
23	Influence of Desorption Conditions on Analyte Sensitivity and Internal Energy in Discrete Tissue or Whole Body Imaging by IR-MALDESI. Journal of the American Society for Mass Spectrometry, 2015, 26, 899-910.	2.8	22
24	SO2 oxidation and nucleation studies at near-atmospheric conditions in outdoor smog chamber. Environmental Chemistry, 2013, 10, 210.	1.5	10
25	Fast response cavity enhanced ozone monitor. Atmospheric Measurement Techniques, 2013, 6, 487-494.	3.1	14
26	Ultra-high resolution and long scan depth optical coherence tomography with full-phase detection for imaging the ocular surface. Clinical Ophthalmology, 2013, 7, 1623.	1.8	2
27	Secondary organic aerosol formation from toluene in an atmospheric hydrocarbon mixture: Water and particle seed effects. Atmospheric Environment, 2011, 45, 2324-2334.	4.1	96
28	Secondary organic aerosol formation from xylenes and mixtures of toluene and xylenes in an atmospheric urban hydrocarbon mixture: Water and particle seed effects (II). Atmospheric Environment, 2011, 45, 3882-3890.	4.1	108
29	The reactive oxidant potential of different types of aged atmospheric particles: An outdoor chamber study. Atmospheric Environment, 2011, 45, 3848-3855.	4.1	90
30	A new gas-phase condensed mechanism of isoprene-NOx photooxidation. Atmospheric Environment, 2011, 45, 4507-4521.	4.1	15
31	The Role of Morphology on Aerosol Particle Reactivity. ACS Symposium Series, 2009, , 13-29.	0.5	0
32	Structure of submonolayer oleic acid coverages on inorganic aerosol particles: evidence of island formation. Physical Chemistry Chemical Physics, 2008, 10, 3156.	2.8	46
33	Ozonolysis of Oleic Acid Adsorbed to Polar and Nonpolar Aerosol Particles. Journal of Physical Chemistry A, 2008, 112, 10315-10324.	2.5	29